ELectronics EXpress

LETTER

IEICE Electronics Express, Vol.12, No.18, 1–6

A novel large-signal model for InP MMIC applications at 110 GHz

Wang Zhi-Ming[a)]**, Luo Xiao-Bin, Zhao Zhuo-Bin, and Lv Xin**

Beijing Key Laboratory of Millimeter Wave and Terahertz Technology,
Beijing Institute of Technology, Beijing 100081, China

a) *wangzhiming872@163.com*

Abstract: This paper presented the development of a novel large-signal equivalent circuit model for InP-based pseudomorphic high electron mobility transistor (PHEMT) MMIC applications beyond 100 GHz. A new set of I-V functions was built in the large-signal model to depict accurately the measured I-V results of this device. The convergence of the model was good during the HB (harmonic balance) simulation. To verify the feasibility of the large-signal model, a 110 GHz MMIC amplifier based on this large-signal model was designed and fabricated, the on-wafer measured large-signal results, which include Pout, Gain and PAE (Power Add Efficiency), were consistent with the simulated ones at 110 GHz. Thus, this new large-signal model has a great potential for InP MMIC applications beyond 100 GHz.

Keywords: large-signal model, SDD, MMIC, InP, PHEMT

Classification: Microwave and millimeter wave devices, circuits, and systems

References

[1] P. Leuther, A. Tessmann, M. Dammann, C. Schworer, M. Schlechtweg, M. Mikulla, R. Losch and G. Weimann: 2007 International Conference on Indium Phosphide and Related Materials (2007) 24. DOI:10.1109/ICIPRM.2007.380680

[2] A. Tessmann: IEEE J. Solid-State Circuits **40** (2005) 2070. DOI:10.1109/JSSC.2005.854591

[3] P. D. Chow, K. Tan, D. Streit, D. Garske, P. Liu and R. Lai: 1992 IEEE MTT-S International Microwave Symposium Digest (1992) 807. DOI:10.1109/MWSYM.1992.188110

[4] W. Deal, X. B. Mei, K. M. K. H. Leong, V. Radisic, S. Sarkozy and R. Lai: IEEE Trans. THz Sci. Technol. **1** (2011) 25. DOI:10.1109/TTHZ.2011.2159539

[5] L. A. Samoska: IEEE Trans. THz Sci. Technol. **1** (2011) 9. DOI:10.1109/TTHZ.2011.2159558

[6] M. Nishimoto, M. Sholley, H. Wang, R. Lai, M. Barsky, D. Streit, Y. Chung, M. Aust, B. Osgood, R. Rajia, C. Gage, T. Gaier and K. Lee: 1999 IEEE Radio Frequency Integrated Circuits (RFIC) Symposium (1999) 99. DOI:10.1109/RFIC.1999.805248

[7] W. Huei, T. N. Ton, K. L. Tan, D. C. Garske, G. S. Dow, J. Berenz, M. W. Pospieszalski and P. S. Shing: IEEE J. Solid-State Circuits **28** (1993) 988. DOI:10.1109/4.237511

DOI: 10.1587/elex.12.20150686
Received August 7, 2015
Accepted August 20, 2015
Publicized September 9, 2015
Copyedited September 25, 2015

[8] J. W. Archer and R. Lai: 2000 Asia-Pacific Microwave Conference (2000) 173. DOI:10.1109/APMC.2000.925753
[9] Z. M. Wang, X. Lv, Z. F. Hu, X. B. Luo, Y. X. Cui, X. G. Sun, J. H. Mo and X. C. Fu: IEICE Electron. Express **3** (2015) 20141174. DOI:10.1587/elex.12.20141174
[10] S. B. Driad, H. Maher, N. Defrance, V. Hoel, J. D. Jaeger, M. Renvoise and P. Frijlink: IEEE Electron Device Lett. **34** (2013) 36. DOI:10.1109/LED.2012.2224313
[11] Z. M. Wang, H. Huang, Z. F. Hu, Z. B. Zhao, X. D. Wang, X. B. Luo, J. Liu, S. Y. Yang and X. Lv: J. Semicond. **36** (2015) 064006. DOI:10.1088/1674-4926/36/6/064006

1 Introduction

In recent years, there has been an increasing demand for MMICs beyond 100 GHz [1, 2]. They are of great interest for high-resolution imaging, environmental sensor, security detection, broadband satellite communication applications [3]. InP-based PHEMTs have shown more excellent performance of high-gain, wide-band, and low noise than the GaAs-based beyond 100 GHz, thus MMICs based on InP PHEMTs have been reported over the world [1, 3, 4, 5, 6, 7, 8].

As the bridge between the device and MMICs, the equivalent circuit models, which include small-signal and large-signal models, play a vital role in the circuit design. Small-signal model is the foundation of large-signal model, and the large-signal model is collections of multiple bias points small-signal models. To some extent, the accuracy of model determines the success of the circuit design. However, many classical and mature large-signal models are suitable for GaAs device. With the development of the InP device technology, it is essential to establish large-signal model special for InP device. In order to satisfy circuit design beyond 100 GHz, the models must depict accurately the device. In this paper, we presented a novel large-signal equivalent circuit model special for InP PHEMT MMIC applications at 110 GHz.

2 Small-signal model

More details about the performance of this InP PHEMT device were described in reference [9]. The 16-element model was used to describe the parasitic and intrinsic parameters up to 110 GHz, which was shown in Fig. 1. The equivalent circuit is commonly shared into an intrinsic section, whose elements are bias dependent, and an extrinsic section, whose values are extracted during pad de-embedding and assumed to be bias independent [10].

The model parameters extractions were based on test structure (PADs) S-parameters and a Cold-FET procedure. Firstly, the PAD capacitances were determined by measuring an open structure that consisted of only the PADs; Secondly, the parasitic inductance and resistance were determined by short structure and a Cold-FET procedure; At last, the intrinsic parameters were extracted after subtracting the parasitic part. More details about the small-signal model of this InP device were described in reference [11].

DOI: 10.1587/elex.12.20150686
Received August 7, 2015
Accepted August 20, 2015
Publicized September 9, 2015
Copyedited September 25, 2015

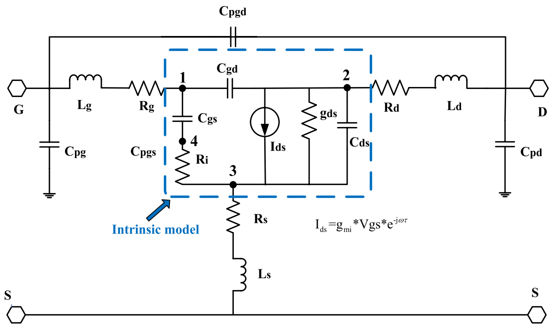

Fig. 1. Small-signal equivalent circuit model

3 Large-signal modeling

The intrinsic model shown in Fig. 1 is bias dependent, it was replaced by a SDD (Symbolically Defined Devices) component with 7 ports in the large-signal model, which was shown in Fig. 2. The SDD relies on the port voltages, currents and their derivatives. Every port of the SDD should be defined by means of equations.

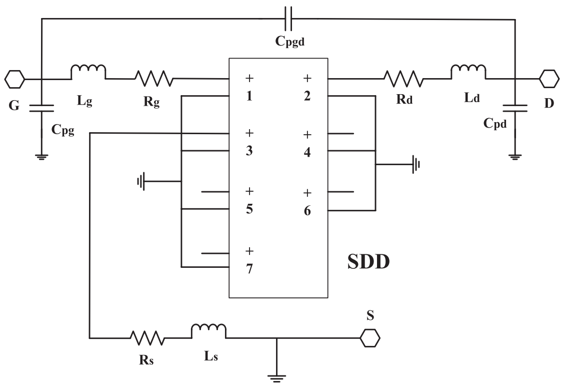

Fig. 2. The large-signal equivalent circuit model implemented by SDD

For the SDD model, the port equations were described as follows:

$$I[1,0] = (\_v5) * Cgd + (\_v6) * Cgs$$

$$I[2,0] = (\_v7) * Cds - (\_v5) * Cgd + (\_v2 - \_v3) * gds$$

$$I[2,2] = Ids - (\_v2)/(Rd + Rs + Rds) \quad H[2] = \exp(-2 * j * pi * freq * t)$$

$$I[3,0] = (\_v4 - \_v3)/Ri - (\_v7) * Cds + (\_v2 - \_v3) * gds$$

$$I[3,2] = -Ids + (\_v2)/(Rd + Rs + Rds) \quad F[4,0] = (\_v6) * Cgs - (\_v4 - \_v3)/Ri$$

$$F[5,1] = \_v1 - \_v2 \quad F[5,0] = -\_v5 \quad F[6,1] = \_v1 - \_v4 \quad F[6,0] = -\_v6$$

$$F[7,1] = \_v2 - \_v3 \quad F[7,0] = -\_v7$$

The drain-source current Ids dependents on the gate and drain voltages. A new set of functions were proposed by taking the feature of InP PHEMT into account. Four sections were used to describe the nonlinear I-V characteristics. The A section was used to describe the transconductance characteristics, B section was to depict the kink effects and C section was for knee voltage feature, respectively. The functions were shown as follows:

ELectronics EXpress

DOI: 10.1587/elex.12.20150686
Received August 7, 2015
Accepted August 20, 2015
Publicized September 9, 2015
Copyedited September 25, 2015

If $Vgs > Vt$, then

$$Ids = A * B * C$$

$$A = a_1 * \tanh(a_2 * (Vgs - Vt)^{a3}) + a_4$$

$$B = b_1 * (Vgs + b_2) * (Vds - b_3) + b_4$$

$$C = c_1 * \tanh(c_2 * \tanh(c_3 * (Vgs - Vt)) * Vds) + c_4$$

Else

$$Ids = d * Vds * gds$$

Where, the Vt stands for the threshold voltage of this device. The $a_1 \sim a_4$, $b_1 \sim b_4$, and $c_1 \sim c_4$ are the fitting coefficients; the d was the leakage current coefficient. Five different Vgs bias points were selected to fit the parameters with Vds varying from 0 to 2 V. The I-V curves comparisons of large-signal model and the measured results were shown in Fig. 3.

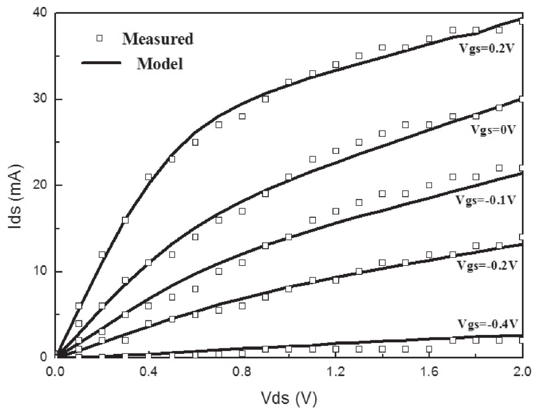

Fig. 3. The DC I-V fitting curves

Different intrinsic parameters were extracted at multiple bias points. They were also expressed to be the functions of Vgs and Vds. The Cgs and Cgd have a great influence to the model so we need to define the C-V fitting expressions. Besides, the other parameters have little impact on the model, so the average values were adopted in the model.

According to the principle of Cgs and Cgd, we build the following equations:

$$Cgs = [e_1 + e_2 * \tanh(Vgs + (Vgs + e_3)^2)] * (e_4 * Vds^2 + e_5 * Vds + e_6) \quad (1)$$

$$Cgd = [f_1 + f_2 * \tanh(Vds + (Vds + f_3)^2)] * (f_4 * Vgs^2 + f_5 * Vgs + f_6) \quad (2)$$

Where, the $e_1 \sim e_6$ and $f_1 \sim f_6$ are the fitting coefficients.

For equation (1), the first part describes Cgs dependence on Vgs, as Vgs varies toward to the pinch off area, the depletion layer becomes deeper, so the Cgs decreases, conversely, the Cgs increases. The second part describes Cgs dependence on Vds, as Vds increases, the depletion layer will become wider, so the Cgs will also increase slightly. The Cgs-V fitting results are shown in Fig. 4.

For equation (2), the first part describes Cgd dependence on Vds, when Vds is low, the gate depletion layer towards drain is shallow, so the Cgd is large, conversely, the Cgd decreases. However, when Vds reaches the saturation region, the Cgd changes slowly or becomes constant with the change of Vds. And the Cgd-V fitting results are shown in Fig. 5.

DOI: 10.1587/elex.12.20150686
Received August 7, 2015
Accepted August 20, 2015
Publicized September 9, 2015
Copyedited September 25, 2015

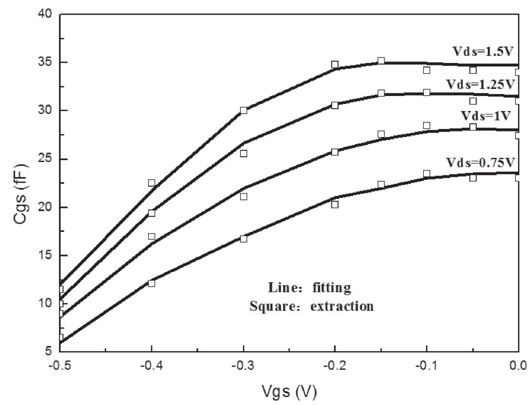

Fig. 4. The Cgs-V fitting results

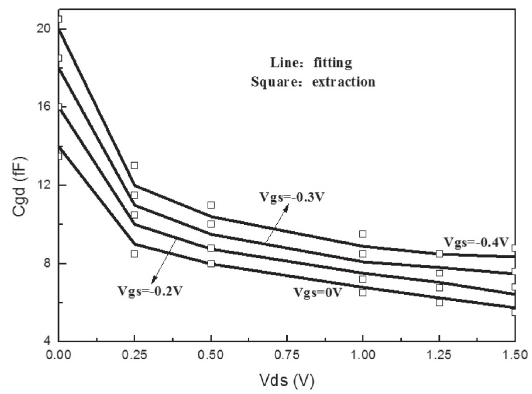

Fig. 5. The Cgd-V fitting results

Meanwhile, the RF S-parameters of this large-signal model would be consistent with the measured results at every bias point from 0.5 to 110 GHz. We took a bias point with Vgs = −0.1 V and Vds = 1.5 V for an instance, the fitting result was shown in Fig. 6.

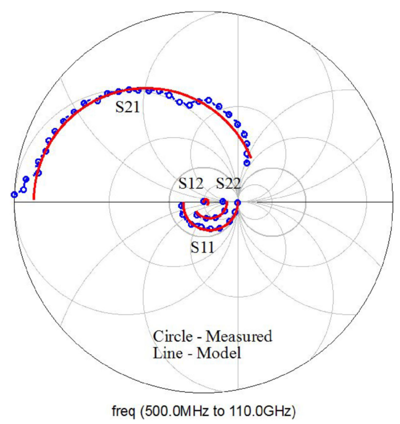

Fig. 6. S-parameters fitting curves from 0.5 to 110 GHz at a bias point

4 Model verification

In order to verify the feasibility of this model, a 110 GHz MMIC amplifier based on the model was designed and fabricated. A photograph of the fabricated MMIC is shown in Fig. 7.

DOI: 10.1587/elex.12.20150686
Received August 7, 2015
Accepted August 20, 2015
Publicized September 9, 2015
Copyedited September 25, 2015

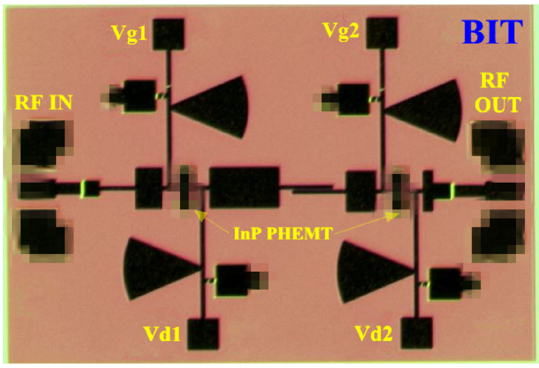

Fig. 7. Chip photograph of the MMIC amplifier

An Agilent PNA-X (N5245A) with frequency extender (75–110 GHz) was used for measurement on-wafer. The power meter was used to calibrate the output power from −20 to 0 dBm at 110 GHz. The simulated large-signal characteristics by harmonic balance were compared with the measured results in Fig. 8.

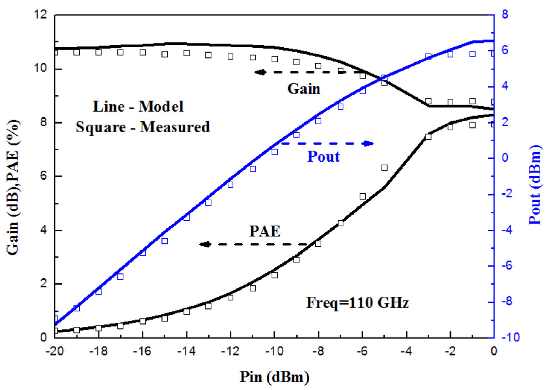

Fig. 8. Large-signal characteristics at Vgs = −0.1 V and Vds = 1.5 V

As shown in Fig. 8, the measured Pout, Gain and PAE curves are accord with the simulated ones. The measured results demonstrate that the Pout is 5.8 dBm, the Gain is compressed from 10.6 to 8.8 dB and the PAE reaches 8% at Pin = 0 dBm. It is proved that this model can be used for MMIC design at 110 GHz. However, there is still some deviation in the simulations, because only about forty bias points were measured to fit the model under the test condition restrictions.

5 Conclusion

A novel large-signal model was presented for InP PHEMT MMIC applications, which was validated at 110 GHz. In the future, multi-way amplifier will be designed to realize high gain and high output power InP MMICs beyond 100 GHz.

Acknowledgement

This research is supported by the National Natural Science Foundation of China (No. 61275107).

DOI: 10.1587/elex.12.20150686
Received August 7, 2015
Accepted August 20, 2015
Publicized September 9, 2015
Copyedited September 25, 2015